Acta Cryst. (1976). B32, 2401

The Crystal Structure of Gladite, $PbCuBi_5S_9$, a Superstructure Intermediate in the Series Bi_2S_3–$PbCuBiS_3$ (Bismuthinite–Aikinite)

BY IWAO KOHATSU* AND B. J. WUENSCH

Department of Materials Science and Engineering, Massachusetts Institute of Technology, Cambridge, Massachusetts 02139, *U.S.A.*

(*Received* 28 *July* 1975; *accepted* 1 *April* 1976)

Gladite, $PbCuBi_5S_9$, is orthorhombic, space group *Pbnm*, with $a=33{\cdot}531$ (6), $b=11{\cdot}486$ (2), $c=4{\cdot}003$ (2) Å, $D_m=6{\cdot}96$ and $D_x=6{\cdot}91$ g cm^{-3} for $Z=4$. Diffraction data were recorded with the multiple-film technique, using graphite-monochromated Ag $K\alpha$ and an integrating precession camera equipped with a masked film cassette, and measured with an automated photoscanner. Gladite is a superstructure with $[a,b,c]=[300/010/001]$ $[a,b,c]$ of bismuthinite, Bi_2S_3. The structure was solved through systematic examination of all configurations permitted by the subcell–supercell relation and refined, by least-squares techniques, to $R=13{\cdot}7\%$ for 1036 observable reflections. The structure is a derivative of Bi_2S_3 in which $\frac{1}{6}$ of the Bi atoms are replaced by Pb, and Cu is added to $\frac{1}{3}$ of a set of available tetrahedral interstices in locations associated with the Pb atoms. In spite of close similarity between the structures of Bi_2S_3 and $PbCuBiS_3$, gladite does not contain a mixture of the four-membered $[Bi_4S_6]$ and $[Pb_2Cu_2Bi_2S_6]$ ribbons found, respectively, in these structures but rather consists of $[Bi_4S_6]$ ribbons alternating along [100] with pairs of a new type of $[PbCuBi_3S_6]$ unit.

Introduction

Several early reports (Lindström 1887, 1889; Flink, 1910; Johansson, 1924) described new Pb–Cu–Bi sulfosalts from a mineral deposit at Gladhammar, Kalmar, Sweden. This locality had been mined for copper in the 18th century and for cobalt in the late 19th century, after which the mine was abandoned. Welin (1966) re-examined material preserved in the Naturhistoriska Riksmuseet, Stockholm, which included several of the original specimens studied by Flink and by Johansson. Through X-ray diffraction and electron microprobe analysis, Welin obtained the first crystal data in support of the validity of several mineral species which had remained incompletely described: gladite, $PbCuBi_5S_9$; hammarite, $Pb_2Cu_2Bi_4S_9$; and $Pb_3Cu_3Bi_7S_{15}$, the latter obtained from the specimen to which Johansson (1924) had earlier ascribed the name lindströmite and the composition $PbCuBi_3S_6$.

The diffraction patterns obtained by Welin from these minerals showed that all were superstructures based upon the structure of bismuthinite, Bi_2S_3 (Hofmann, 1933; Kupčík & Veselá-Nováková, 1970). One cell dimension was equal to three, three and five times that of a translation in Bi_2S_3 for $PbCuBi_5S_9$, $Pb_2Cu_2Bi_4S_9$ and $Pb_3Cu_3Bi_7S_{15}$ respectively. Aikinite, $PbCuBiS_3$, is a derivative of the bismuthinite structure (Wickman, 1953; Ohmassa & Nowacki, 1970*a*; Kohatsu & Wuensch, 1971) in which one-half of the metal atoms in the four-membered ribbons of the Bi_2S_3 structure are replaced by Pb atoms, and Cu atoms are added to all available positions in a set of tetrahedral interstices between ribbons. It thus appeared likely that the intermediate members of the Bi_2S_3–$PbCuBiS_3$ series consisted of ordered structures in which the Bi atoms in bismuthinite were only partially replaced by Pb, and in which the available interstices were only partially occupied by Cu atoms. A classification of bismuthinite derivatives was proposed on this basis by Moore (1967) and compositions were predicted for an extensive list of hypothetical derivatives. The present structural investigation of gladite was performed (Kohatsu, 1971) to confirm these apparent relations and provide insight into the structural basis for the formation of such superstructures. A summary of the results has already been presented (Kohatsu & Wuensch, 1972, 1973*a*).

Experimental

Material and X-ray examination

The sole crystal of gladite which was known was that isolated by Welin (1966). This specimen (Swedish Museum Catalogue No. RM 24097) was kindly transmitted to us for study through Professor P. B. Moore. The crystal had a shape close to a parallelepiped with dimensions $0{\cdot}076\times0{\cdot}181\times0{\cdot}508$ mm. However, features such as a large conchoidal chip missing from one surface ($0{\cdot}181\times0{\cdot}508$ mm) rendered this description of the specimen only approximate in subsequent corrections for absorption. It was considered imprudent to attempt to reduce the dimensions of the crystal or to grind it into a more regular shape in view of the unique nature of the sample.

Buerger-precession and Weissenberg photographs

* Present address: Chevron Research Company, Richmond, California, U.S.A.

showed the crystal to be orthorhombic with diffraction symbol *mmmPbn*–. This permits *Pbnm* (D_{2h}^{16}) or $Pbn2_1$ (C_{2v}^{9}) as possible space groups. The centrosymmetric space group subsequently proved satisfactory for analysis of the structure. The diffracted intensities were strong and comparable to reflections obtained from bismuthinite when $h=3n$, thus confirming the superstructure relation found by Welin (1966).

Precise lattice constants were obtained by least-squares fit to 137 *hk*0 and 30 0*kl* reflections recorded with the aid of a back-reflection Weissenberg camera. The computer program employed (Burnham, 1962) allowed refinement of parameters characterizing systematic errors due to shrinkage, absorption, and sample eccentricity. The lattice constants obtained (Table 1) are in good agreement with those reported by Welin (1966). The experimental density of 6·96 g cm^{-3} (Johansson, 1924) is close to the density of 6·91 g cm^{-3} computed for ideal $PbCuBi_5S_9$.

Table 1. *Comparison of lattice constants for bismuthinite* (Bi_2S_3), *gladite* ($PbCuBi_5S_9$) *and aikinite* ($PbCuBiS_3$)

λ(Cu $K\alpha_1$) = 1·54051Å; estimated standard deviations are in parentheses.

	Bismuthinite (i)	Gladite (ii)	Gladite (iii)	Aikinite (iv)
a	11·115 (20)	33·66 = 3 × 11·22	33·531 (6) = 3 × 11·177 (2)	11·2754 (17)
b	11·25 (2)	11·45	11·486 (2)	11·6083 (10)
c	3·97 (1)	4·02	4·003 (2)	4·0279 (3)

References: (i) Kupčík & Veselá-Nováková (1970). (ii) Welin (1966). (iii) Present work. (iv) Kohatsu & Wuensch (1971).

Intensity collection

Gladite has a very high linear absorption coefficient. The dimensions of the sole crystal available for study made attractive the use of a short-wavelength radiation to minimize absorption effects. Graphite-monochromated Ag $K\alpha$ radiation ($\mu_l = 384$ cm^{-1}) was thus employed. This radiation reduced $\mu_l r_{max}$ to 3·49, but dictated the use of photographic techniques for data collection in order to resolve the closely spaced maxima.

Intensities were recorded with an integrating precession camera. A film cassette which had been equipped with a rotating mask (Wuensch & Thomas, 1971) was employed to eliminate one of the two reflections which comprise each spot on a normal precession film. This permitted use of the multiple-film technique by preventing the overlap and interference which would have resulted from 'doubling' of the closely spaced reflections on those films in the pack which could not be correctly positioned. Sheets of 0·001in Cu foil were inserted between films to reduce transmission to the order of 0·38 to 0·51, depending upon the level being recorded.

Photographs were recorded for levels *h*0*l* through *h*5*l*, and for *hk*0 through *hk*2. An integration motion of about 1 mm was employed along the direction of **c*** on the *b* axis photographs, but none could be employed along **a*** because of the extremely close spacing of reflections. No integrating motion was used for the *c* axis photographs. The intensities were measured with the aid of an automatic photoscanner (Photoscan System P-1000, Optronics International Inc., Chelmsford, Massachusetts) which recorded optical densities and coordinates on magnetic tape. A computer program was written by I. Kohatsu to obtain intensity along selected columns on each level. The *b* axis films which had been mechanically integrated in one dimension along **c*** were integrated along **a*** by manual computation. The scans of the *c* axis precession films were integrated along **b*** by the computer program; these integrands were manually summed along **a***.

Only 1036 of the 2430 accessible reflections were detectable, of which 441 were the weaker superstructure reflections ($h \neq 3n$). The observable intensities were corrected for absorption, Lorentz and polarization effects with *QUAC*, a version of the program *ACAC* (Wuensch & Prewitt, 1965) modified by J. J. Kohatsu to include Gaussian quadrature integration, modification of the polarization factor for monochromation, and modification of the standard Lorentz factor for the precession motion to take into account the fact that (in these experiments) the only reflections recorded were those generated as the reciprocal lattice points moved *into* the sphere of reflection.

Solution of the structure

Gladite was anticipated to have the same arrangement of heavy atoms and sulfur atoms as bismuthinite and aikinite, and to differ from the latter structure primarily through the number and arrangement of Cu atoms. However, a complement-structure Patterson function (Buerger, 1959), synthesized from the superstructure reflections alone, did not reveal strong positive maxima at locations consistent with possible Cu positions. The predominant features of the maps were instead adjacent positive and negative peaks at locations such as $(\frac{1}{3},0,0)$ and $(\frac{1}{6},\frac{1}{2},0)$. These indicated that the principal contributions to the superstructure intensities came from displacements, especially of the heavy atoms, along **a**, the direction of formation of the superstructure.

The structure was solved through systematic consideration of all models permitted by the substructure-superstructure relation. There are, in general, several distinct settings for a substructure in a supercell (Wuensch, 1969). Space group *Pbnm* of the bismuthinite substructure has eight independent inversion centers, each of which might be placed in coincidence with the inversion center at the origin of the *Pbnm* supercell. Since only the *a* axis of the supercell differs from the translations of the subcell, these possibilities differ only by a shift in origin and the setting of the subcell is uniquely determined.

Using only the heavy-metal atoms, with Bi assigned to all positions and with all atoms assigned a temperature factor of 1·0 Å^2, a single scale factor and atomic positions were varied – first with the substructure reflections and then the superstructure reflections alone. The next step was to locate the sites occupied by Cu atoms. Three distributions were possible (Fig. 1) if it is assumed that the Cu atoms are located in a fraction of the set of tetrahedral interstices which are occupied in aikinite. The Cu atoms were added to the structure-factor computations, and each of the three possible models was refined, as above, with only the superstructure reflections. The refinement converged to R values of 28·7 and 28·1% for Cu in the B and C sites, respectively, but 22·3% for occupancy of the A site. It may be noted that the A sites represent the most widely separated set of positions permitted by the space group. Addition of nine S atoms to the asymmetric unit (initially at locations derived from the aikinite subcell) and further refinement reduced R for the superstructure reflections only slightly to 21·0% (the metal atoms account for 78% of the scattering density in the cell). For all reflections R was 18·2%. The bond lengths between the metal and S atoms were then computed. Of distances between the six heavy-metal atoms (all arbitrarily treated as Bi to this stage) and their closest S atom neighbor, five fell between 2·61 and 2·69 Å, distances which are normal for Bi–S separations. The sixth separation was 2·90 Å and this heavy-metal atom could clearly be designated Pb.

Refinement of the structure

Anomalous scattering corrections were introduced for all atoms once the site occupied by Pb had been identified. Examination of the agreement between F_o and F_c revealed abnormal discrepancies for several weak intensities: F_o was more than $10F_c$. All of these reflections (24 in number) occurred close to the periphery of the film where the background was increasing rapidly, and where a background could not be measured about the complete perimeter of the reflection. These structure factors were accordingly removed from the data set. Further refinement of the positional parameters resulted in a decrease of R to 17·1%. All reflections had been assigned equal weights in refinement to this stage. An evaluation of $|F_o-F_c|$ as a function of F_o showed the difference to be a weak function of F_o. In subsequent refinement the weight assigned to reflections was adjusted such that $w(F_o-F_c)^2$ was constant and independent of the magnitude of F_o. With incorporation of the revised weighting scheme isotropic temperature factors were adjusted for all atoms and R converged to 16·1%.

A difference map prepared at this stage revealed evidence for slight anisotropic thermal motion of the heavy-metal atoms. No interpretable anomalies occurred near the location of the Cu and S atoms. Introduction and refinement of anisotropic temperature factors for the heavy-metal atoms provided a slightly improved R value of 15·6%. Anisotropic temperature factors were then employed for the S and Cu atoms as well, but no significant improvement in the value of R was obtained. To this point in the refinement only a single scale factor had been employed for the nine different levels of photographically recorded data (six levels normal to **b*** and three levels normal to **c***). Introduction and refinement of separate scale factors for these individual levels reduced the value of R to 14·8%. After adjustment of the separate scale factors, the atomic positions and anisotropic temperature factors were varied for all atoms. No significant changes occurred. The final value of R was 13·7% for 1036 observable structure factors. The 'weighted' R, $[\sum w(F_o-F_c)^2/\sum wF_o^2]^{1/2}$, was 19·1%. With inclusion of 1333 unobservable structure factors, at values equal to $1/\sqrt{3}$ of the estimated minimum observable value, R became 24·4%.

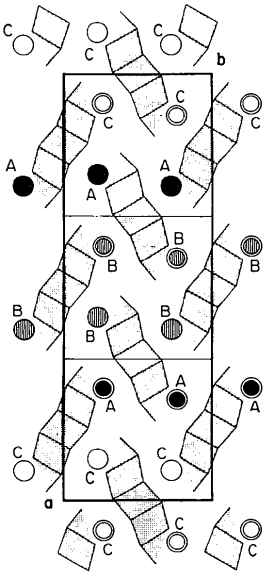

Fig. 1. The three possible sets of tetrahedral interstices (among four-membered bismuthinite-like ribbons) which are available for the Cu atom in gladite (double circles indicate sites at $z=\frac{3}{4}$, single circles sites at $z=\frac{1}{4}$).

Discussion of the structure

The asymmetric unit of the gladite structure contains 16 atoms: Pb, Cu, five Bi and nine S atoms, all located in special position 4(*c*)*m* of space group *Pbnm*. The final atomic positions and anisotropic temperature factor coefficients are presented in Tables 2 and 3 respectively.† Interatomic distances, interbond angles

† Lists of axes of thermal ellipsoids and structure factors have been deposited with the British Library Lending Division as Supplementary Publication No. SUP 31781 (18 pp., 1 microfiche). Copies may be obtained through The Executive Secretary, International Union of Crystallography, 13 White Friars, Chester CH1 1NZ, England.

Table 2. *Atom positions for gladite* ($\times 10^4$) *and displacements from ideal bismuthinite- and aikinite-like configurations* (Å $\times 10^3$)

z for all atoms is $\frac{1}{4}$; estimated standard deviations are in parentheses.

	Gladite			Bismuthinite				Aikinite		
	x	y		$a\Delta x$	$b\Delta y$	Displacement		$a\Delta x$	$b\Delta y$	Displacement
Bi(1)	565 (1)	209 (5)	Bi(1)	−54	+49	73	Bi	−131	+28	134
Bi(2)	3924 (2)	56 (5)	Bi(1)	+34	−126	131	Bi	−44	−148	154
Bi(3)	7294 (2)	283 (5)	Bi(1)	+154	+134	205	Bi	+77	+113	136
Bi(4)	6550 (2)	3542 (5)	Bi(2)	−10	+156	156	Pb	−258	+241	353
Bi(5)	9866 (1)	3430 (5)	Bi(2)	−67	+28	72	Pb	−315	+113	335
Pb	3349 (2)	3174 (5)	Bi(2)	+433	−266	508	Pb	+188	−181	261
Cu	2390 (5)	2200 (14)		–	–	–	Cu	+101	−138	171
S(1)	2095 (8)	354 (25)	S(1)	0	−148	148	S(1)	−97	−115	150
S(2)	5415 (11)	552 (31)	S(1)	−44	+79	90	S(1)	−144	+113	183
S(3)	8804 (10)	565 (29)	S(1)	+141	+94	169	S(1)	+44	+128	135
S(4)	1855 (8)	3786 (30)	S(2)	−3	+41	41	S(2)	+13	−10	17
S(5)	5172 (10)	3760 (30)	S(2)	−57	+11	58	S(2)	−40	−40	57
S(6)	8511 (11)	3917 (34)	S(2)	−40	+192	196	S(2)	−24	+140	142
S(7)	1006 (7)	2158 (21)	S(3)	−50	−23	55	S(3)	−20	+14	24
S(8)	4344 (11)	2038 (34)	S(3)	−33	−161	164	S(3)	−3	−124	124
S(9)	7669 (11)	2290 (34)	S(3)	−64	+129	144	S(3)	−34	+165	169

and S–S atom separations in the metal-atom coordination polyhedra are presented in Table 4.* Corresponding data for the S atom coordination polyhedra are summarized in Table 5. The thermal motion of the metal atoms was found to be only moderately anisotropic. The thermal motion of all S atoms was isotropic within experimental error. This, in combination with the high standard deviation of β_{ij} in the presence of heavy-metal atoms, caused the standard deviations of the orientation angles to be several times larger than the magnitudes of the individual values.

* In Table 4 and the subsequent discussion a superscript is used to designate an atom related by symmetry to an atom in the asymmetric unit. The value of this integer corresponds to the position of the coordinates of the atom in the list of equivalent positions presented for space group *Pbnm* in *International Tables for X-ray Crystallography* (1952). Atoms equivalent by translation are not distinguished.

Table 3. *Anisotropic temperature factor coefficients*

$\beta_{23}=\beta_{13}=0$ for all atoms, and $T=\exp[-(h^2\beta_{11}+k^2\beta_{22}+l^2\beta_{33}+2hk\beta_{12})]$. Estimated standard deviations are in parentheses.

	β_{11} ($\times 10^5$)	β_{22} ($\times 10^4$)	β_{33} ($\times 10^3$)	β_{12} ($\times 10^5$)	Equivalent isotropic temperature factor (Å$^2\times 10^2$)
Bi(1)	25 (4)	20 (3)	11 (4)	10 (8)	96 (10)
Bi(2)	30 (3)	27 (3)	16 (4)	7 (10)	125 (10)
Bi(3)	45 (5)	16 (3)	10 (3)	−5 (9)	116 (9)
Bi(4)	34 (4)	33 (4)	19 (4)	18 (11)	150 (9)
Bi(5)	19 (4)	25 (3)	19 (3)	2 (9)	114 (9)
Pb	20 (4)	28 (3)	20 (3)	−22 (10)	122 (9)
Cu	12 (13)	5 (9)	6 (11)	2 (29)	40 (26)
S(1)	19 (24)	14 (17)	10 (20)	−11 (53)	74 (48)
S(2)	41 (33)	31 (25)	30 (32)	−8 (66)	179 (74)
S(3)	22 (26)	27 (22)	20 (25)	7 (54)	122 (59)
S(4)	8 (21)	11 (15)	11 (19)	4 (44)	55 (44)
S(5)	26 (27)	28 (21)	22 (27)	4 (60)	136 (62)
S(6)	46 (35)	35 (25)	20 (30)	−16 (71)	174 (73)
S(7)	1 (19)	5 (14)	1 (16)	−4 (38)	13 (39)
S(8)	39 (32)	34 (25)	39 (37)	−6 (70)	203 (74)
S(9)	45 (36)	37 (26)	28 (32)	6 (73)	192 (57)

A projection of the structure of gladite along **c** is presented in Fig. 2. The structure is composed of four-membered ribbons similar to those which are found in the structures of bismuthinite, Bi_2S_3, and stibnite, Sb_2S_3. The ribbons, however, are of two types. The first, delineated by bold hatching, is identical with the $[Bi_4S_6]$ slab which is found in Bi_2S_3. The second ribbon, indicated by lighter shading, has composition $[PbCuBi_3S_6]$. This unit is a hybrid between the $[Bi_4S_6]$ ribbon of Bi_2S_3, and the $[Pb_2Cu_2Bi_2S_6]$ ribbon which constitutes the structure of aikinite, $PbCuBiS_3$. It is of interest to note that the interstitial site occupied by Cu turns out to be coupled to the position occupied by Pb in exactly the same fashion as in aikinite.

The structure of gladite thus consists of a combination of $[PbCuBi_3S_6]$ and $[Bi_4S_6]$ quadruple ribbons in the ratio 2:1. Ohmasa & Nowacki (1970*b*) had independently employed subgroup–supergroup relations to enumerate the configurations possible for the structure of gladite. Their considerations showed that the structure could theoretically be comprised of combinations of either bismuthinite-like, aikinite-like, or $PbCuBi_3S_6$ units. As only bismuthinite-like and aikinite-like units were then known to exist, the structures which consisted of mixtures of bismuthinite and aikinite chains were considered to be the practical possibilities. The present results show this not to be the case.

Previous comparison of the structures of bismuthinite and aikinite (Kohatsu & Wuensch, 1971) has shown the atomic coordinates to be remarkably similar in spite of the replacement of one-half of the Bi atoms by Pb in aikinite, and the addition of interstitial Cu atoms. The length and width of the $[Bi_4S_6]$ and $[Pb_2Cu_2Bi_2S_6]$ ribbons are nearly identical, and the

atomic array in aikinite is essentially that of bismuthinite homogenously expanded by 1·5% in directions normal to the 4 Å lattice constant. The slight difference in size nevertheless appears sufficient to cause the Pb atom in gladite to order among the maximum permissible number of chains.

The metal-atom coordination polyhedra in gladite are compared with those of bismuthinite and aikinite in Fig. 3. The figure is arranged so that the polyhedra of the $[Bi_4S_6]$ chain in gladite are adjacent to the corresponding polyhedra in bismuthinite, while those of the aikinite-like end of the $[PbCuBi_3S_6]$ slab adjoin the corresponding polyhedra of aikinite. All the heavy-metal atoms in the structure of bismuthinite and its derivatives have S atom neighbors at positions close to five of the six vertices of an octahedron. The metal atom is appreciably displaced from the base of this square pyramid, as may be seen in Fig. 2. Sixth and seventh S atom neighbors are present at larger distances in locations which constitute a 'split vertex' for an octahedral configuration. The plane formed by the metal atom and the two atoms of the 'split vertex' bisects two of the bond angles in the base of the square pyramid. The metal-atom coordination polyhedra are distorted and are of two distinct types. The exterior Bi atom in the bismuthinite chain has three close neighbors at approximately equal distances which, together with Bi, form the trigonal pyramid which is characteristic of the lighter Group V elements. Two additional S atoms and one atom of the split vertex are at larger and similar distances and complete a distorted [3+3] octahedral coordination. The first row of Fig. 3 shows that the corresponding polyhedra in gladite and aikinite retain this character.

Table 4. *Interatomic distances and bond angles in the metal-atom coordination polyhedra*

Estimated standard deviations are in parentheses, closest second-nearest atom in brackets. The metal atom following the sulfur–sulfur atom separation indicates the polyhedron, if any, which shares that edge.

Metal	M–S(*i*) (Å)		S(*i*)–M–S(*j*) (°)		S(*i*)–S(*j*) (Å)	
Bi(1)	S(5^3)	2·67 (2) 2×	S(5^3)–S(5^4)	80·7 (9) 2×	3·66 (6)	Bi(1^2)
	S(7)	2·69 (3)	S(3^2)–S(3^2)	82·1 (8)	4·00 (0)=*c*	Pb^4
	S(5^4)	2·97 (3)	S(3^2)–S(7)	82·1 (7) 2×	3·78 (3)	Bi(4^3)
	S(3^2)	3·05 (2) 2×	S(5^3)–S(7)	84·4 (8) 2×	3·60 (3)	
	[S(8^4)	3·65 (4)]	S(3^2)–S(5^4)	88·9 (7) 2×	4·02 (5)	Bi(1)
			S(5^3)–S(5^3)	97·0 (11)	4·00 (0)=*c*	Bi(5)
			S(3^2)–S(5^4)	114·4 (7) 2×	3·84 (4)	
Bi(2)	S(8)	2·68 (4)	S(4^4)–S(6^3)	76·2 (9) 2×	3·53 (4)	Bi(3^2)
	S(6^3)	2·70 (3) 2×	S(2^2)–S(8)	79·4 (9) 2×	3·68 (5)	Bi(5^3)
	S(4^4)	3·00 (3)	S(2^2)–S(2^2)	81·5 (9)	4·00 (0)=*c*	Bi(5^4)
	S(2^2)	3·07 (3) 2×	S(6^3)–S(8)	84·3 (10) 2×	3·61 (4)	
	[S(7^4)	3·33 (2)]	S(2^2)–S(6^3)	89·2 (8) 2×	4·06 (5)	Bi(2)
			S(6^3)–S(6^3)	95·7 (12)	4·00 (0)=*c*	Pb
			S(2^2)–S(4^4)	121·4 (7) 2×		
Bi(3)	S(9)	2·63 (4)	S(4^3)–S(6^4)	74·3 (7) 2×	3·53 (4)	Bi(2^2)
	S(4^3)	2·70 (2) 2×	S(1^2)–S(9)	83·3 (8) 2×	3·88 (4)	Pb^3
	S(1^2)	2·96 (2) 2×	S(4^3)–S(9)	85·0 (8) 2×	3·60 (4)	Cu^3
	S(6^4)	3·11 (4)	S(1^2)–S(1^2)	85·2 (8)	4·00 (0)=*c*	Bi(4^4)
	[S(9^4)	3·44 (4)]	S(1^2)–S(4^3)	88·5 (6) 2×	3·95 (4)	Bi(3)
			S(4^3)–S(4^3)	95·5 (9)	4·00 (0)=*c*	Bi(4)
			S(1^2)–S(6^4)	118·5 (7) 2×		
Bi(4)	S(3^4)	2·61 (3)	S(1^3)–S(1^3)	84·0 (8)	4·00 (0)=*c*	Bi(3^4)
	S(7^3)	2·83 (2) 2×	S(1^3)–S(3^4)	84·2 (8) 2×	3·77 (3)	Pb^2
	S(1^3)	2·99 (2) 2×	S(3^4)–S(7^3)	87·8 (7) 2×	3·78 (3)	Bi(1^3)
	[S(4^3)	3·49 (2) 2×]	S(7^3)–S(7^3)	90·1 (7)	4·00 (0)=*c*	
			S(1^3)–S(7^3)	92·4 (5) 2×	4·18 (5)	Bi(4)
Bi(5)	S(2^4)	2·61 (4)	S(2^3)–S(2^4)	81·7 (10) 2×	3·65 (6)	Bi(5^2)
	S(8^3)	2·72 (3) 2×	S(2^3)–S(2^3)	85·0 (10)	4·00 (0)=*c*	Bi(2^4)
	S(2^3)	2·96 (3) 2×	S(2^4)–S(8^3)	87·3 (10) 2×		Bi(2^3)
	[S(5^3)	3·38 (3) 2×]	S(2^3)–S(8^3)	89·1 (8) 2×	3·99 (5)	Bi(5)
			S(8^3)–S(8^3)	94·8 (12)	4·00 (0)=*c*	
Pb	S(3^3)	2·90 (2) 2×	S(6^3)–S(9^3)	65·5 (9) 2×	3·38 (5)	
	S(1^4)	2·91 (3)	S(1^4)–S(9^3)	76·8 (7) 2×	3·88 (4)	Bi(3^3)
	S(9^3)	3·07 (3) 2×	S(6^3)–S(6^3)	77·9 (10)	4·00 (0)=*c*	Bi(2)
	S(6^3)	3·18 (3) 2×	S(1^4)–S(3^3)	80·8 (7) 2×	3·77 (3)	Bi(4^2)
	[S(8)	3·57 (4)]	S(9^3)–S(9^3)	81·3 (4)	4·00 (0)=*c*	Cu
			S(3^3)–S(6^3)	81·6 (7) 2×	3·98 (4)	
			S(3^3)–S(3^3)	87·3 (8)	4·00 (0)=*c*	Bi(1^4)
			S(3^3)–S(9^3)	91·4 (7) 2×		Pb
			S(6^3)–S(9^3)	113·8 (10) 2×		Bi(3^2)
Cu	S(9^3)	2·29 (2) 2×	S(4) –S(9^3)	96·2 (11) 2×	3·60 (4)	Bi(3^3)
	S(1)	2·34 (3)	S(1) –S(4)	110·5 (12)	3·95 (4)	Bi(4^3)
	S(4)	2·55 (3)	S(1) –S(9^3)	114·0 (10) 2×	3·72 (4)	Bi(3^2)
	[S(9)	4·01 (3)]	S(9^3)–S(9^3)	121·9 (19)	4·00 (0)=*c*	Pb

The interior Bi atom of the bismuthinite chain has a different coordination. The apical bond length is the shortest, and is significantly smaller than the minimum separation in the [3+3+1] coordinated Bi atom. The second and third nearest neighbors are at larger distances than in the Bi(1) group, while the fourth and fifth are closer. The coordination of Bi(2) in bismuthinite is thus [1+2+2+2]. Fig. 3 shows the interior bismuth atom, Bi(5), of the $[Bi_4S_6]$ ribbon in gladite to have an almost identical set of interatomic distances. The coordination about Bi(4) in gladite, the interior Bi at the bismuthinite-like end of the $[CuPbBi_3S_6]$ ribbon, is essentially the same but minor distortions created by the substitution of Pb in this unit cause the correspondence to be less exact. The Pb coordination group in gladite is similar to that in aikinite. The Cu atom has tetrahedral coordination as in aikinite, but the bond distances are more irregular. The Cu coordination in gladite almost approaches triangular coordination: the sum of the bond angles for the three shortest bonds is 349·9 rather than 328·4° as in a regular tetrahedron. Also, the Cu–S(9) distance of 2·29 Å is almost comparable with the 2·20–2·27 Å range of separations found for CuS_3 triangles in structures such as those of tetrahedrite and tennantite (Wuensch, Takéuchi & Nowacki, 1966).

The S atom polyhedra in gladite are contrasted with corresponding units in bismuthinite and aikinite in Fig. 4. The correspondence between these groups is less exact because the absence or presence of interstitial Cu and substituted Pb in differing amounts causes the number and type of nearest metal neighbors to be quite different. However, in some cases [*e.g.* S(1) in gladite and aikinite] the interatomic distances are in even closer agreement than for the metal-atom polyhedra. This is especially the case when all neighbors are the same [*e.g.* S(1) in bismuthinite and S(2) in gladite; S(3) in bismuthinite and S(7) and S(8) in gladite].

There is an interesting similarity between the thermal motions of the substituted Pb atoms in gladite and aikinite. Both the largest and the smallest principal axes of vibration [0·251 (4) and 0·128 (4) Å for aikinite (Kohatsu & Wuensch, 1971) compared with 0·144 (8) and 0·097 (12) Å for gladite] for this atom lie normal to the 4 Å lattice translation, and the minimum principal axis is oriented toward the interstitial Cu atom. Specifically, the angle between *a* and the smallest thermal axis is 24 (9)° for gladite, 22·6 (1·1)° for aikinite, while the orientation of the Cu–Pb interatomic vector is 19·2°.

Table 2 compares the distortion of the atomic positions in gladite from the ideal locations of bismuthinite-like and aikinite-like arrays of atoms. The positions of the S atoms remain remarkably similar. The displacements range from only 0·041–0·196 Å (mean

Table 5. *Interatomic distances and bond angles in the sulfur-atom coordination polyhedra*

Estimated standard deviations are in parentheses, second-nearest neighbor distances in brackets.

	S–M(*i*) (Å)		M(*i*)–S–M(*j*) (°)			
S(1)	Cu	2·34 (3)	Cu—Bi(4^3)	82·8 (8) 2×	Bi(4^3)–Pb^4	93·0 (2) 2×
	Pb^4	2·91 (3)	Bi(4^3)–Bi(4^3)	84·0 (8)	Bi(3^2)–Bi(4^3)	94·3 (2) 2×
	Bi(3^2)	2·96 (2) 2×	Bi(3^2)–Bi(3^2)	85·2 (8)	Bi(3^2)–Pb^4	98·1 (8) 2×
	Bi(4^3)	2·99 (2) 2×	Cu—Bi(3^2)	86·1 (8) 2×		
S(2)	Bi(5^4)	2·61 (4)	Bi(2^2)–Bi(2^2)	81·5 (9)	Bi(2^2)–Bi(5^3)	95·6 (2) 2×
	Bi(5^3)	2·96 (3) 2×	Bi(5^3)–Bi(5^3)	85·0 (10)	Bi(5^3)–Bi(5^4)	98·3 (10) 2×
	Bi(2^2)	3·07 (3) 2×	Bi(2^2)–Bi(5^4)	92·8 (9) 2×		
S(3)	Bi(4^4)	2·61 (3)	Bi(1^2)–Bi(1^2)	82·1 (8)	Bi(1^2)–Pb^3	93·3 (2) 2×
	Pb^3	2·90 (2) 2×	Pb^3—Pb^3	87·3 (8)	Bi(4^4)–Pb^3	101·8 (9) 2×
	Bi(1^2)	3·05 (2) 2×	Bi(1^2)–Bi(4^4)	93·1 (7) 2×		
S(4)	Cu	2·55 (3)	Bi(4^3)–Bi(4^3)	70·0 (5)	Bi(3^3)–Bi(3^3)	95·5 (9)
	Bi(3^3)	2·70 (2) 2×	Cu—Bi(4^3)	70·2 (6) 2×	Bi(2^4)–Bi(4^3)	96·7 (7) 2×
	Bi(2^4)	3·00 (3)	Cu—Bi(3^3)	84·5 (7) 2×	Bi(2^4)–Bi(3^3)	106·2 (7) 2×
	[Bi(4^3)	3·49 (2) 2×]	Bi(3^3)–Bi(4^3)	92·2 (3) 2×		
S(5)	Bi(1^3)	2·67 (2) 2×	Bi(5^3)–Bi(5^3)	72·7 (7)	Bi(1^3)–Bi(1^4)	99·3 (9) 2×
	Bi(1^4)	2·97 (3)	Bi(1^3)–Bi(5^3)	92·1 (3) 2×	Bi(1^4)–Bi(5^3)	99·5 (8) 2×
	[Bi(5^3)	3·38 (3) 2×]	Bi(1^3)–Bi(1^3)	97·0 (11)		
S(6)	Bi(2^3)	2·70 (3) 2×	Pb^3—Pb^3	77·9 (10)	Bi(2^3)–Bi(3^4)	103·3 (10) 2×
	Bi(3^4)	3·11 (4)	Pb^3—Bi(2^3)	87·1 (4) 2×	Pb^3—Bi(3^4)	103·4 (9) 2×
	Pb^3	3·18 (3) 2×	Bi(2^3)–Bi(2^3)	95·7 (12)		
S(7)	Bi(1)	2·69 (3)	Bi(4^3)–Bi(4^3)	90·1 (7)	Bi(1) –Bi(2^4)	150·7 (10)
	Bi(4^3)	2·83 (2)	Bi(1) –Bi(4^3)	96·7 (7) 2×		
	[Bi(2^4)	3·33 (2)]	Bi(2^4)–Bi(4^3)	103·8 (6) 2×		
S(8)	Bi(2)	2·68 (4)	Bi(5^3)–Bi(5^3)	94·8 (12)		
	Bi(5^3)	2·72 (3) 2×	Bi(2) –Bi(5^3)	99·0 (11) 2×		
	[Pb	3·57 (4)]				
	[Bi(1^4)	3·65 (4)]				
S(9)	Cu^3	2·29 (2) 2×	Cu^3—Bi(3^4)	76·0 (10) 2×	Pb^3—Bi(3^4)	98·5 (9) 2×
	Bi(3)	2·63 (4)	Cu^3—Pb^3	77·3 (6) 2×	Pb^3—Bi(3)	101·8 (10) 2×
	Pb^3	3·07 (3) 2×	Pb^3—Pb^3	81·3 (8)	Cu^3—Cu^3	121·9 (19)
	[Bi(3^4)	3·44 (4)]	Cu^3—Bi(3)	91·4 (11) 2×		

0·118 Å) and 0·017–0·183 Å (mean 0·111 Å) relative to bismuthinite and aikinite respectively. The displacements of the metal atoms are of comparable magnitude when a given site is occupied by the same species: 0·072–0·205 Å (mean 0·127 Å) for Bi positions in gladite relative to Bi sites in bismuthinite, 0·134–0·154 Å (mean 0·141 Å) for Bi positions common to gladite and aikinite, and 0·261 Å relative to the site occupied by Pb in aikinite. Distortions are considerably larger if coordinates of sites occupied by different metal atoms are compared: The Pb atom in gladite is displaced 0·51 Å from the ideal location of Bi(2) in bismuthinite, and the atoms Bi(4) and Bi(5) in gladite are displaced 0·335 and 0·353 Å relative to corresponding positions of the Pb atom in aikinite.

The atomic coordinates in gladite thus differ by amounts of only *ca* 0·1 Å from the ideal locations in homogeneously expanded structures of bismuthinite or aikinite when a given position is occupied by the same chemical species. If different metal atoms occupy the positions under comparison, the distortions are roughly three times larger, and may amount to as much as 0·5 Å.

The largest distortion by far of the atomic positions in aikinite relative to those in bismuthinite was shown (Kohatsu & Wuensch, 1971) to be that of the substituted Pb atom (0·259 Å). The greatest component of this displacement was along the direction corresponding to **a** in Fig. 2. The effect may reflect, in part, the larger Pb–S(3) separation in aikinite, relative to Bi(2)–S(3) in bismuthinite but it may also indicate a repulsive interaction between Pb and the associated interstitial Cu atom. The displacement of the Pb atom in gladite relative to Bi in bismuthinite is 0·503 Å – nearly twice as large as in aikinite. This difference cannot be explained in terms of substitution of an atom with slightly larger bond distances. Inspection of Fig. 2 shows that gladite, in comparison with aikinite, lacks an interstitial Cu on the opposite side of the Pb atom [which would be present at $z=\frac{3}{4}$ between Pb and S(8)]. If a repulsive interaction indeed exists between Cu and Pb, the absence of the balancing force from the vacant Cu site would allow the Pb atom to be displaced further along **a**. This would appear to be a plausible explanation for the larger distortion. The details of the distortion of atomic positions in bismuthinite derivatives from the parent structure thus arise, in part, from the substitution of a heavy-metal atom with larger nearest-neighbor separations and partially from interactions between the substituted species.

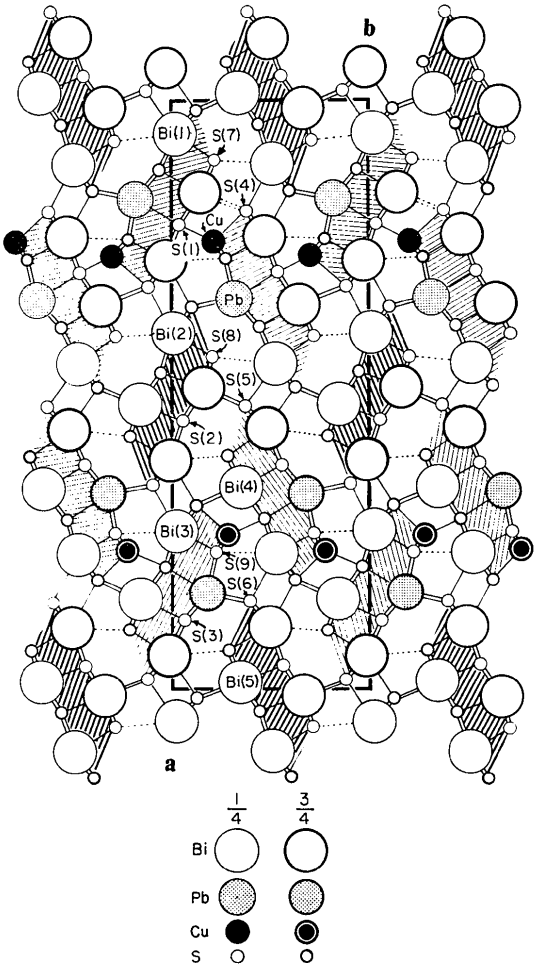

Fig. 2. A projection of the structure of gladite along **c**. Bonds indicated by a single line are to an atom with the same *z* coordinate. Double lines represent bonds to a pair of translation-equivalent atoms which superpose in projection. The structure is composed of $[Bi_4S_6]$ ribbons identical with those in bismuthinite (heavy hatching) and a new type of $[CuPbBi_3S_6]$ ribbon (light hatching).

Epilogue

When this study was completed (Kohatsu, 1971) the sole crystal of gladite known was the specimen isolated by Welin (1966). Many of the experimental procedures employed in the present study were dictated by this circumstance. Attempts to synthesize ordered bismuthinite derivatives have, to date, proved fruitless at temperatures as low as 300°C (Springer, 1971). Gladite has been identified from two additional localities since the completion of this work: at Krupka in the Krušnéhory Mountains in Northwestern Bohemia (Syneček & Hybler, 1974) and in the Tennant Creek deposits, Northern Territory, Australia (Mumme &

Table 6. *Comparison of crystal data for gladite from recently discovered localities*

	Gladhammar (i)	Krupka (ii)	Tennant Creek (iii)
a	33·531 (6) Å	33·62 Å	33·546 Å
b	11·486 (2)	11·48	11·498
c	4·003 (2)	4·00	4·001

References: (i) Present work. (ii) Syneček & Hybler (1974). (iii) Mumme, to be published.

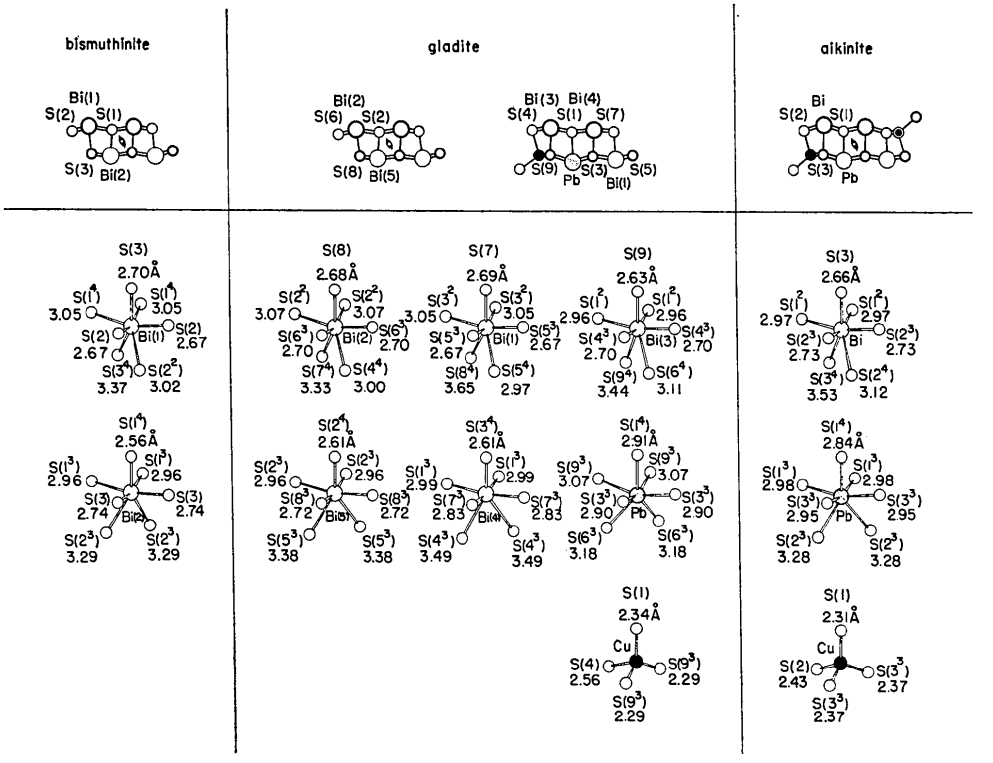

Fig. 3. Comparison of the metal-atom coordination polyhedra found in gladite with those which occur in bismuthinite (Kupčík & Veselá-Nováková, 1970) and aikinite (Kohatsu & Wuensch, 1971). Corresponding polyhedra in the three structures are grouped in rows. The metal atoms in the $[Bi_4S_6]$ ribbon of gladite are adjacent to those of bismuthinite, and those at the aikinite-like end of the $[CuPbBi_3S_6]$ ribbon are adjacent to aikinite.

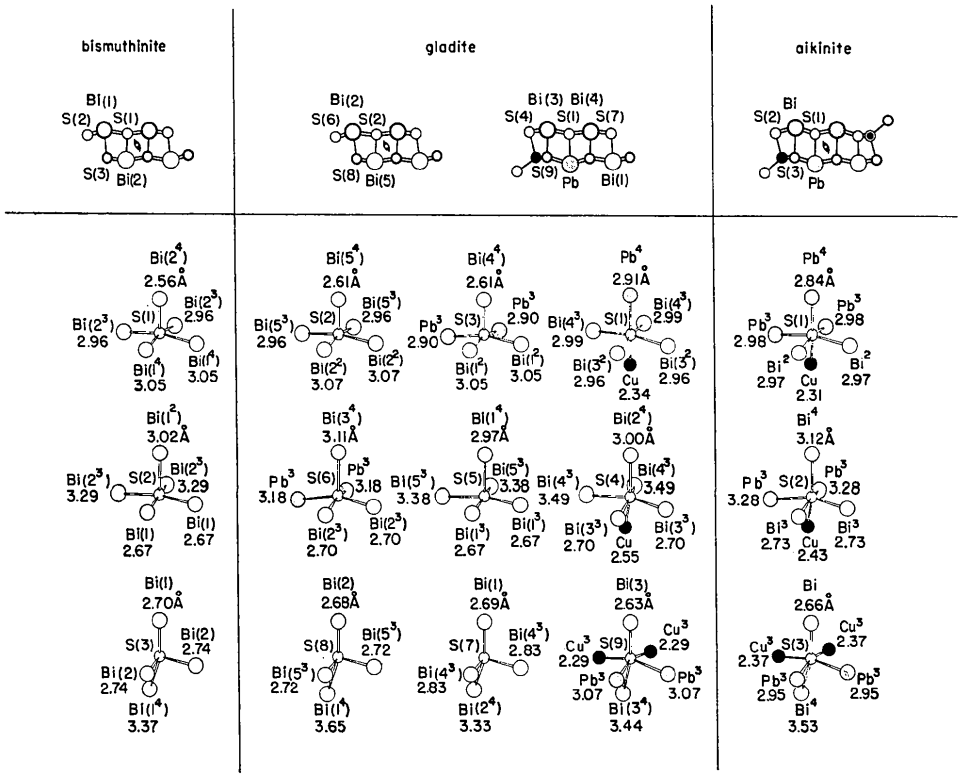

Fig. 4. Comparison of the sulfur-atom coordination polyhedra found in gladite with those which occur in bismuthinite and aikinite. The polyhedra are arranged on the same basis as in Fig. 3.

Watts, to be published). The lattice constants obtained from these new samples correspond well with the values obtained in this study (Table 6). Syneček & Hybler (1974) conducted an independent preliminary study of the structure of Krupka gladite in projection along **c** ($R=25\%$). The atomic arrangement is the same as that obtained in the present study. The atomic coordinates (given to only three figures) differ by several standard deviations from the values reported here.*

The new $[PbCuBi_3S_6]$ ribbon which has been found in gladite was reported by us earlier (Kohatsu & Wuensch, 1973*b*) in connection with a discussion of the chain-like units found in bismuth-rich Pb–Bi sulfosalts. Two additional superstructures have very recently been discovered. Pekoite, $PbCuBi_{11}S_{18}$, (Mumme & Watts, to be published) has a supercell of the same geometry as that of gladite and consists of $[PbCuBi_3S_6]$ and $[Bi_4S_6]$ ribbons in the ratio 1:2. Discovery of krupkaite, $PbCuBi_3S_6$, and solution of the structure was reported simultaneously by separate investigators (Žák, Syneček & Hybler, 1974; Syneček & Hybler, 1974; Mumme, 1975). Krupkaite has a cell similar to that of bismuthinite and aikinite, but has a space group of lower symmetry ($Pb2_1m$). The structure consists entirely of $[PbCuBi_3S_6]$ ribbons. Such units appear to play a dominant role in the crystal chemistry of the bismuthinite derivatives. Since a parent structure is now known which consists entirely of $[PbCuBi_3S_6]$ units, it appears resonable to refer to the ribbon of this composition which was found in gladite as a 'krupkaite ribbon' (Mumme, Welin & Wuensch, 1976).

The authors are indebted to Professor P. B. Moore for making the unique crystal of Gladhammar gladite available for study, and to Dr Eric Welin for continued interest in the problem. The study was supported by grants GA-22698Al and DES74-12826 from the Earth Sciences Section of the U.S. National Science Foundation. The contribution of one of us (I.K.) was supported, in part, by an IBM Fellowship.

* The average differences Δx and Δy for the heavy-metal atoms and S atoms, respectively, are 0·0003 and 0·0037, and 0·0029 and 0·0073. Relative to the standard deviations of the present study, the corresponding average values of Δ/σ for these quantities are 2·22 and 7·33, and 2·99 and 2·46.

References

BUERGER, M. J. (1959). *Vector Space.* New York: John Wiley.

BURNHAM, C. W. (1962). *Carnegie Inst. Wash. Yearb.* **61**, 133–135.

FLINK, G. (1910). *Ark. Mineral. Geol.* **3**, 1–166.

HOFMANN, W. (1933). *Z. Kristallogr.* **86**, 225–245.

International Tables for X-ray Crystallography (1952). Vol. I. Birmingham: Kynoch Press.

JOHANSSON, K. (1924). *Ark. Mineral. Geol.* **9**, 1–22.

KOHATSU, I. (1971). Ph. D. Thesis, Dept. of Metallurgy and Materials Science, Mass. Inst. of Tech.

KOHATSU, I. & WUENSCH, B. J. (1971). *Acta Cryst.* B**27**, 1245–1252.

KOHATSU, I. & WUENSCH, B. J. (1972). Program and Abstracts, Winter Meet., Amer. Cryst. Assoc., 36.

KOHATSU, I. & WUENSCH, B. J. (1973*a*). *Amer. Min.* **58**, 1098.

KOHATSU, I. & WUENSCH, B. J. (1973*b*). *Z. Kristallogr.* **138**, 343–365.

KUPČÍK, V. & VESELÁ-NOVÁKOVÁ, L. (1970). *Mineral. Petrogr. Mitt.* **14**, 55–59.

LINDSTRÖM, G. (1887). *Geol. Fören. Stockh. Förh.* **9**, 523–528.

LINDSTRÖM, G. (1889). *Geol. Fören. Stockh. Förh.* **11**, 171–172.

MOORE, P. B. (1967). *Amer. Min.* **52**, 1874–1876.

MUMME, W. G. (1975). *Amer. Min.* **60**, 300–308.

MUMME, W. G., WELIN, E. & WUENSCH, B. J. (1976). *Amer. Min.* **61**, 15–20.

OHMASA, M. & NOWACKI, W. (1970*a*). *Z. Kristallogr.* **132**, 71–86.

OHMASA, M. & NOWACKI, W. (1970*b*). *Neues Jb. Mineral. Mh.* pp. 158–162.

SPRINGER, G. (1971). *Neues Jb. Mineral. Mh.* pp. 19–24.

SYNEČEK, V. & HYBLER, J. (1974). *Neues Jb. Mineral. Mh.* pp. 541–560.

WELIN, E. (1966). *Ark. Mineral. Geol.* **4**, 377–386.

WICKMAN, F. E. (1953). *Ark. Mineral. Geol.* **1**, 501–507.

WUENSCH, B. J. (1969). *Acta Cryst.* A**25**, S86.

WUENSCH, B. J. & PREWITT, C. T. (1965). *Z. Kristallogr.* **122**, 24–59.

WUENSCH, B. J., TAKÉUCHI, Y. & NOWACKI, W. (1966). *Z. Kristallogr.* **123**, 1–20.

WUENSCH, B. J. & THOMAS, R. L. (1971). *J. Appl. Cryst.* **4**, 204–207.

ŽÁK, L., SYNEČEK, V. & HYBLER, J. (1974). *Neues Jb. Mineral. Mh.* pp. 533–541.